

Electronic Supporting Information for:

Benzimidazole-embedded *N*-fused aza-indacenes: Synthesis and deprotonation-assisted optical detection of carbon dioxide†

Masatoshi Ishida,^{a,b} Pyosang Kim,^a Jiyoung Choi,^c Juyoung Yoon,^{c*} Dongho Kim^{a*} and Jonathan L. Sessler^{a,d*}

^a*Department of Chemistry, Yonsei University, Shinchon-dong 134, Seodaemun-gu, Seoul, 120-749, Korea. Fax: (+82)-2-2123-2434; Email: dongho@yonsei.ac.kr*

^b*Department of Chemistry and Biochemistry, Kyushu University, Fukuoka 819-0395, Japan.*

^c*Department of Chemistry and Nano Science and Department of Bioinspired Science, Ewha Womans University, Seoul 120-750,*

Korea. E-mail: jyoon@ewha.ac.kr

^d*Department of Chemistry & Biochemistry, 105 E. 24th Street - Stop A5300, University of Texas at Austin, Austin, Texas 78712-1224, United States. Fax: (+1) 512-471-5009; E-mail: sessler@cm.utexas.edu*

Table of Contents

Instruments and materials

Synthetic procedures

X-ray diffraction analyses

Hirshfeld surface analyses

Theoretical calculations

Spectroscopic measurements

Supporting figures and tables

Determination of equilibrium constants

Experimental section:

Instruments: ^1H -NMR and ^{13}C -NMR spectra were recorded on a Bruker Avance II (400 MHz for ^1H , 100 MHz for ^{13}C) spectrometer and ^{19}F -NMR spectra were recorded on a JEOL JNM-AL300 (282 MHz) spectrometer. Chemical shifts (δ) are referenced to residual non-deuterated dichloromethane (5.32 ppm for ^1H -NMR spectra, 53.80 ppm for ^{13}C -NMR); CF_3COOH (-76.55 ppm) was used as internal standard for the ^{19}F -NMR spectral analyses. High-resolution mass (HRMS) spectra were obtained using a JEOL LMS-HX-110 spectrometer with 3-nitrobenzyl alcohol (NBA) as the matrix. UV-vis absorption spectra were recorded on a SCINCO S-4100 photodiode array spectrometer. Fluorescence spectra were recorded on a SCINCO FS-2 spectrophotometer. Time-resolved fluorescence lifetimes were determined using the time-correlated single-photon-counting (TCSPC) technique. As an excitation light source, a Ti:sapphire laser (Mai Tai BB, SpectraPhysics), which provides a repetition rate of 800 kHz with ~ 100 fs pulses generated by a homemade pulse-picker, was used. The output pulse of the laser was frequency-doubled using a 1 mm thick second harmonic crystal (β -barium borate, BBO, CASIX). The fluorescence was collected by a microchannel plate photomultiplier (MCP-PMT, Hamamatsu, R3809U-51) with a thermoelectric cooler (Hamamatsu, C4878) connected to a TCSPC board (Becker&Hickel SPC-130). The overall instrumental response function was about 25 ps (the full width at half maximum (fwhm)). A vertically polarized pump pulse produced by means of a Glan-laser polarizer was used to irradiate the samples, while a sheet polarizer, set at an angle complementary to the magic angle (54.7°), was placed in the fluorescence collection path to obtain polarization-independent fluorescence decays.

Materials. Unless otherwise noted, reagents of the best available grade were purchased from commercial suppliers and used without further purification. Pyrrole was purified by distillation *in vacuo*. Solvents were used after appropriate distillation or purification. Analytical thin-layer chromatography (TLC) was performed on Merck silica gel 60 pre-coated aluminum sheets. Column chromatography was carried out using silica gel 60N (60 mesh, KANTO Chemical Co.) or neutral

alumina (Wako Chemical Co.).

Synthetic procedures

5,6-Dichloro-1H-benzo[d]imidazol-2-yl-phenylmethanol (3): This compound was prepared using a modified literature procedure.^{S1} Briefly, 5,6-dichloro-1,2-phenylenediamine (1.0g, 5.68 mmol) and D,L-mandelic acid (0.95 g, 6.25 mmol) were suspended in 20 mL of H₂O containing 3 mL of conc. HCl solution. The resulting mixture was heated at reflux for 4 h, and then cooled to room temperature. Aqueous NaHCO₃ was then added to neutralize the solution. The white precipitate that resulted was collected by filtration and washed with CHCl₃ several times. Yield: 0.68 g, 2.32 mmol (41%). ¹H-NMR (400 MHz, CDCl₃) δ 7.66 (s, 2H, NH+OH), 7.48 (d, $J = 7.8$ Hz, 2H, Ph-H), 7.34 (t, $J = 7.8$ Hz, 2H, Ph-H), 7.28 (d, $J = 7.8$ Hz, 1H, Ph-H), 6.72 (s, 2H, phenylene-H), 5.96 (s, 1H, CH) ppm. HR-MS (FAB) $m/z = 293.0245$ (found), 293.0248 (calcd for C₁₄H₁₁N₃Cl₂O).

Compound 1: Compound **3** (200 mg, 0.68 mmol) and pyrrole (20 equiv) were dissolved in dry MeCN (30 mL). An excess of trifluoroacetic acid (0.4 mL) was added dropwise into the mixture, which was then stirred while heating to reflux for 48 h under a nitrogen atmosphere. The color of the solution became increasingly reddish brown as the reaction progressed. After allowing the reaction mixture to cool to room temperature, 2,3-dichloro-5,6-dicyano-1,4-benzoquinone (DDQ, 0.46 g, 2.05 mmol) was added. The reaction mixture was then stirred for 1 h. The solvent was removed *in vacuo*, and the resulting black tarry residue was passed through an Al₂O₃ column eluting with CHCl₃ so as to collect the yellow fraction. The crude product obtained in this way was further purified by column chromatography over silica gel eluting with CHCl₃ containing 0.5% MeOH. The highly green fluorescent fraction obtained from this column was collected and found to be **1**. Yield: 5 mg, 11.9 μ mol (2%) ¹H-NMR (400 MHz, CD₂Cl₂) δ 8.42 (br s, 2H, NH+Ar-H), 7.99 (s, 1H, Ar-H), 7.82 (d, $J = 7.1$ Hz, 2H, Ph-H), 7.63 (t, $J = 7.5$ Hz, 2H, Ph-H), 7.56 (d, $J = 7.7$ Hz, 1H, Ph-H), 7.50 (s, 1H,

Pyrr-H), 6.82 (s, 1H, Pyrr-H) ppm. No reliable ^{13}C -NMR spectrum of this derivative could be obtained due to the inherent molecular aggregation and resulting low solubility in all deuterated solvents available for testing (*vide infra*). ^{19}F -NMR (282 MHz, CDCl_3) δ -59.19 (s, 3F, CF_3) ppm. HR-MS (FAB) m/z = 419.0206 (found), 419.0204 (calcd for $\text{C}_{20}\text{H}_{10}\text{N}_3\text{Cl}_2\text{F}_3$). UV-vis (MeCN): λ_{max} [nm] ($\log \epsilon$ [$\text{M}^{-1}\text{cm}^{-1}$]) = 309 (4.56), 357 (3.82), 442 (3.89), 4.67 (3.88). Elemental analysis: C 58.44; H 1.97; N 10.22% (found); $\text{C}_{20}\text{H}_{10}\text{Cl}_2\text{F}_3\text{N}_3$ requires C 57.16; H 2.40; N 10.00% (calcd).

Compound 2: This compound was prepared using reaction conditions similar to those used to prepare **1**. In this case, the reaction of **3** (200 mg, 0.68 mmol) 1-ethyl-3-(3-dimethylaminopropyl) carbodiimide hydrochloride (EDC, 273 mg, 1.43 mmol) with indole (96 mg, 0.82 mmol) in 30 mL of MeCN containing excess TFA (0.4 mL) afforded a brown colored solution. After the addition of DDQ (0.46 g, 2.05 mmol) a reddish solution was obtained. After stirring for 1 h, the crude product was purified by chromatography over first Al_2O_3 (CHCl_3 , eluent) and then silica gel (CHCl_3 containing 0.5% MeOH, eluent). The highly yellow fluorescent fraction from the latter column was collected and taken to dryness to give 12 mg, 25.6 μmol (4%) of **2**. The NMR spectra of **2** were recorded in the presence of TFA to prevent intermolecular interactions. ^1H -NMR (400 MHz, CD_2Cl_2 +TFA) δ 9.30 (s, 1H, NH), 8.49 (s, 1H, Ar-H), 8.44 (d, J = 8.5 Hz, 1H, Indo-H), 8.00 (s, 1H, Ar-H), 7.72-7.79 (m, 6H, Ph-5H+Indo-H), 7.55 (t, J = 7.8 Hz, 1H, Indo-H), 7.53 (t, J = 7.8 Hz, 1H, Indo-H); ^{13}C -NMR (100 MHz, CD_2Cl_2 +TFA) δ 145.27, 144.24, 143.51, 134.38, 133.19, 132.56, 131.61, 130.84, 129.90, 128.73, 127.64, 126.98 (q, J = 9.3Hz, $\underline{\text{C}}\text{-CF}_3$), 126.75, 123.74, 121.28 (q, J = 274.2Hz, CF_3), 115.66, 112.73, 107.01; ^{19}F -NMR (283 MHz, CD_2Cl_2 + TFA) δ -59.21 (s, 3F, CF_3) ppm. HR-MS (FAB) m/z = 469.0355 (found), 469.0360 (calcd for $\text{C}_{24}\text{H}_{12}\text{N}_3\text{Cl}_2\text{F}_3$). UV-vis (MeCN): λ_{max} [nm] ($\log \epsilon$ [$\text{M}^{-1}\text{cm}^{-1}$]) = 315 (4.64), 457 (3.58), 482 (3.56). Elemental analysis: C 60.92; H 2.78; N 8.40 (found); $\text{C}_{24}\text{H}_{12}\text{N}_3\text{F}_3\text{Cl}_2$ requires C 61.30; H 2.57; N 8.94% (calcd).

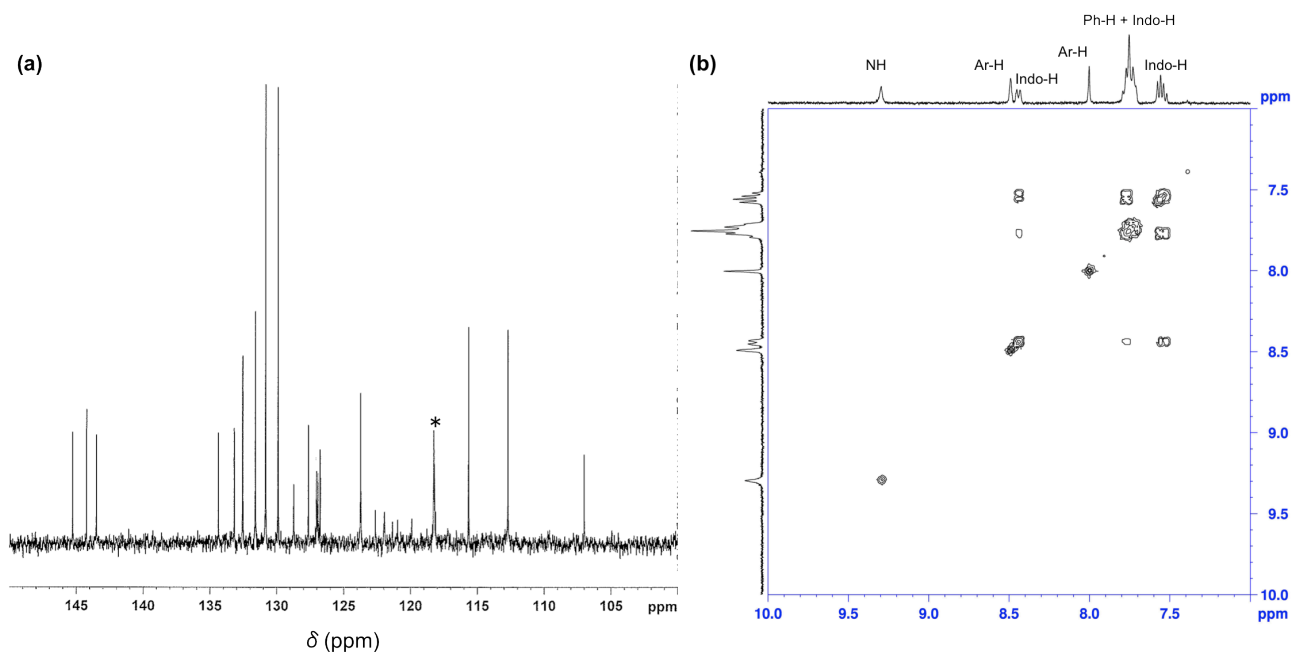


Figure S1. (a) Partial ^{13}C NMR and (b) ^1H - ^1H COSY spectra of the protonated form of **2** as recorded in CD_2Cl_2 in the presence of TFA at 298 K. The asterisk indicates the residual TFA solvent peak.

X-ray diffraction analyses. The X-ray structures of **1** and **2** were determined using a Rigaku RAXIS rapid imaging plate area detector with graphite-monochromated $\text{MoK}\alpha$ radiation ($\lambda = 0.71075 \text{ \AA}$). The data crystals were mounted on a glass fiber. The data for **1** ($2\theta = 54.8^\circ$) and **2** ($2\theta = 54.9^\circ$) were collected at 133K. The raw data were corrected for both Lorentz and polarization effects. The structures were solved by direct methods and refined anisotropically for the non-hydrogen atoms via full-matrix least-squares calculations. The hydrogen atoms were located at the calculated positions. They were assigned a fixed displacement and constrained to an ideal geometry with $\text{C-H} = 0.95 \text{ \AA}$ except for the N-H hydrogen atoms. The thermal parameters of the calculated hydrogen atoms were related to those of their parent atoms by $U(\text{H}) = 1.2U_{\text{eq}}(\text{C})$. Crystallographic calculations were performed using the Crystal Structure Software package of the Rigaku Corporation.^{S2} Crystallographic data for **1**• CHCl_3 : $\text{C}_{21}\text{H}_{11}\text{N}_3\text{Cl}_5\text{F}_3$, $M_w = 539.60$, monoclinic, space group $P2_1/c$, $a = 11.068(3)$, $b = 8.982(3)$, $c = 21.773(7) \text{ \AA}$, $\beta = 92.46(3)^\circ$, $V = 2162(1) \text{ \AA}^3$, $Z = 4$, $D_{\text{calc}} = 1.657 \text{ g/cm}^3$, $F_{000} = 1080.00$, $R_1 (I > 2.00\sigma(I)) = 0.0375$, $wR_2 (\text{All data}) = 0.0930$, GOF = 0.942. Further details of

the structure are available from the Cambridge Crystallographic Data center by quoting CCDC no: 940145. Crystallographic data for **2**; C₂₄H₁₂N₃Cl₂F₃, M_w = 469.0360, *monoclinic*, Space Group *P2₁/c*, *a* = 8.186(2), *b* = 10.575(2), *c* = 22.441(4) Å, *β* = 91.64 (9) °, *V* = 1942.0(6) Å³, *Z* = 4, *D_{calc}* = 1.608 g/cm³, *F₀₀₀* = 452.00, *R₁* (*I* > 2.00σ (*I*)) = 0.0338, *wR₂* (All data) = 0.0819, GOF = 1.036. Further details of the structure are available from the Cambridge Crystallographic Data center by quoting CCDC no: 940146.

Hirshfeld surface analyses: Hirshfeld surfaces^{S3} and the associated 2D-fingerprint plots^{S4} were calculated using *CrystalExplorer*, which accepts a structure input file in CIF format. Bond lengths to hydrogen atoms were set to typical neutron values (C-H = 1.083 Å, N-H = 1.009 Å). For each point on the Hirshfeld isosurface, two distances, namely *d_e*, the distance from the point to the nearest nucleus external to the surface and *d_i*, the distance to the nearest nucleus internal to the surface, were defined. The normalized contact distance (*d_{norm}*) based on *d_e* and *d_i* is given by:

$$d_{norm} = (d_i - r_i^{vdW}) / r_i^{vdW} + (d_e - r_e^{vdW}) / r_e^{vdW}$$

where *r_i^{vdW}* and *r_e^{vdW}* are the van der Waals radii of the atoms. The value of *d_{norm}* is negative or positive depending on whether the intermolecular contacts are shorter or longer than the van der Waals separations. The parameter *d_{norm}* defines a surface with a red-white-blue color scheme, where bright red spots highlight shorter contacts, white areas represent contacts around the van der Waals separation, and blue regions are devoid of close contacts.

Theoretical calculations. All calculations were carried out with the Gaussian 03 software package.^{S5} Energy calculations for, and geometry optimizations of, compounds **1** and **2** were performed using the hybrid B3LYP DFT method employing the 6-31G(d,p) basis set without any symmetry restriction.^{S6} The optimized geometries were then used to carry out time dependent (TD)-DFT calculations of the excited-state energies and oscillator strengths using the 6-31+G(d,p) basis set and electron population analyses using the 6-31G(d,p) basis set. All molecular orbitals were visualized with the software GaussView 4.1.

Spectroscopic measurements: Stock solutions of **1** and **2** were prepared in dry MeCN (1.0×10^{-5} M). Solutions containing salts of various anions were prepared in absolute MeCN and at a defined concentration. The solutions of **1** and **2** were charged into a 1 cm long quartz cell, and the stock solution of the anion salts were added into the quartz cell dropwise using a micro-syringe. The fluorescent quantum yields were determined relative to a rhodamine 6G standard ($\Phi_f = 0.95$ in EtOH).^{S7}

Determination of equilibrium constants: To determine the equilibrium constants corresponding to reaction of **1** and **2** with the fluoride anion (K_s), the absorption intensity changes were analyzed by nonlinear curve fitting assuming a 1:1 reaction:

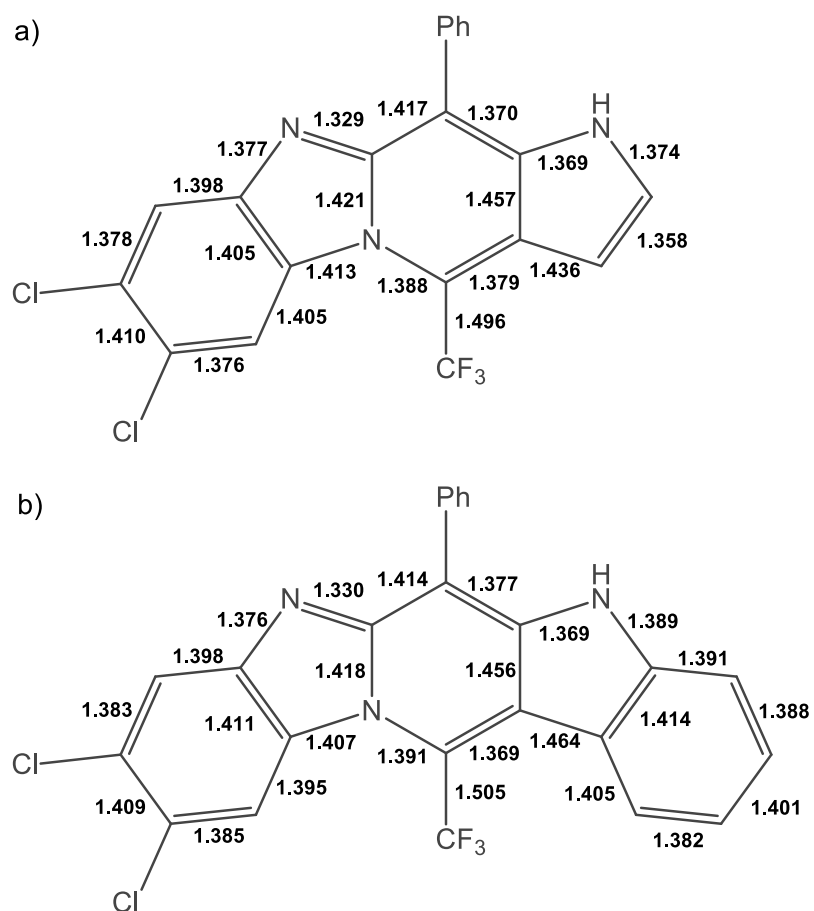
$$A/A_0 = 1 + (A_{max} / 2A_0 - 1/2) \{1 + C_M/C_L + 1/K_S C_L - [(1 + C_M/C_L + 1/K_S C_L)^2 - 4C_M/C_L]^{1/2}\}$$

where A and A_0 are the absorbance intensities of the receptor in question recorded in the presence and absence of anions, F^- ; C_M and C_L are the concentrations of F^- and **1** (or **2**); K_S is the equilibrium constant.

Table S1. Photophysical properties of **1** and **2** recorded at 298 K

Compd	Solvent	λ_{abs} (nm) ^a	λ_{em} (nm) ^b	Stokes shift (cm^{-1})	Φ_{fl} ^c	τ (ns) ^d	$k_{fl}(10^7 s^{-1})$ ^e	$k_{nr}(10^7 s^{-1})$ ^e
1	CH ₂ Cl ₂	468	493	1083	0.88	19.4	4.55	0.62
	THF	474	492	772	0.53	16.4	3.24	2.87
	acetone	470	491	910	0.54	15.2	3.56	3.03
	MeCN	465	490	1143	0.66	15.4	4.29	2.24
	EtOH	464	487	1018	0.72	16.0	4.51	1.76
2	CH ₂ Cl ₂	482	522	1590	0.71	23.9	2.97	1.21
	THF	493	527	1309	0.48	22.3	2.15	2.33
	acetone	488	526	1480	0.46	21.3	2.16	2.54
	MeCN	482	524	1663	0.53	21.1	2.51	2.24
	EtOH	481	520	1559	0.58	22.0	2.64	1.91

^aLowest energy absorption band maxima. ^bFluorescence emission band maxima observed upon excitation at 370 nm. ^cFluorescence quantum yields. ^dFluorescence lifetime as measured by the TCSPC method ($\lambda_{ex} = 370$ nm). ^eCalculated rate constants for fluorescence and nonradiative decay.



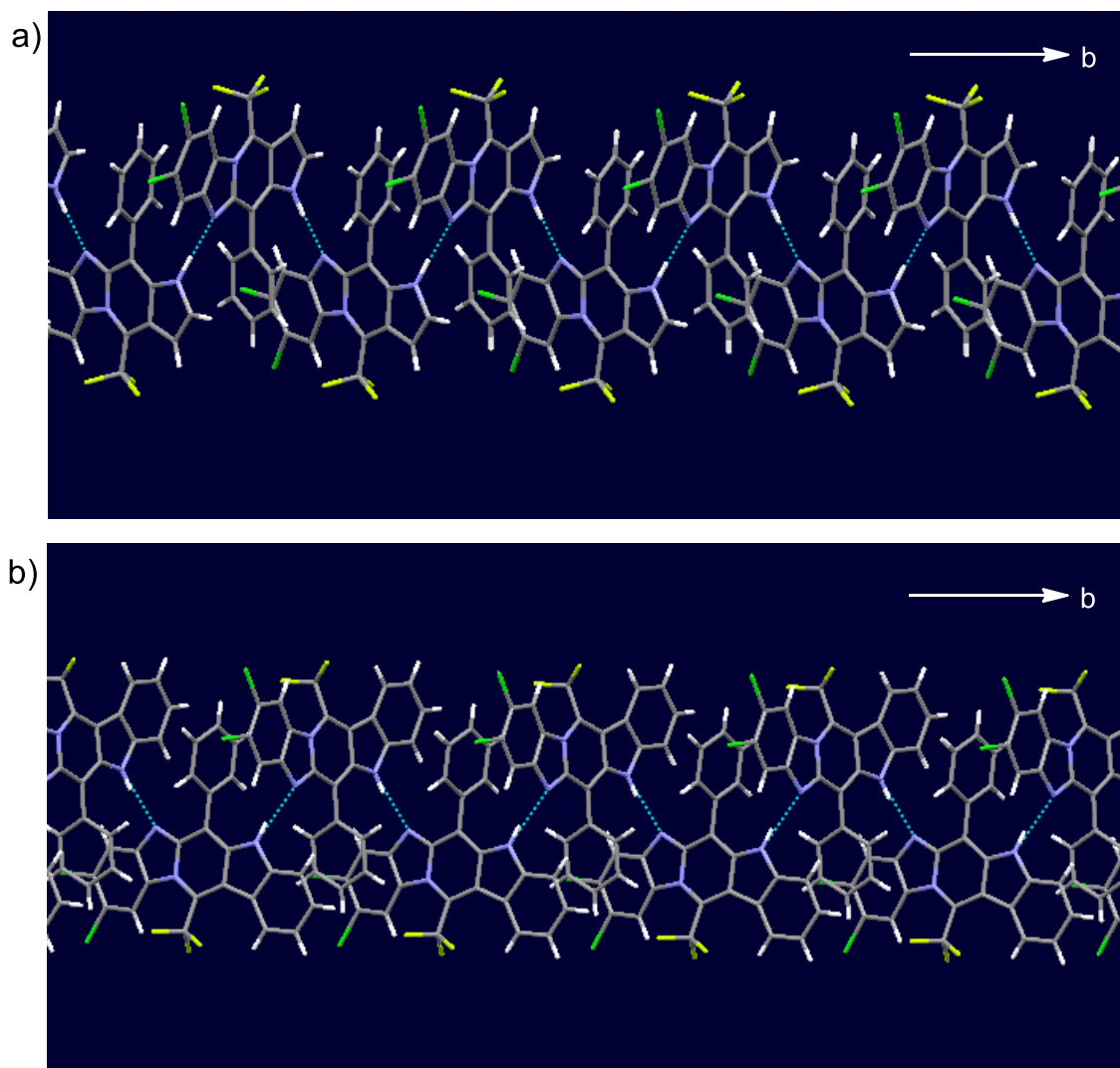


Figure S3. Crystal packing of compounds a) **1** and b) **2** revealing the arrangement along the *b*-axis of the respective lattices. The colors of each atom are as follows: gray (carbon), yellow (fluorine), blue (nitrogen), green (chlorine), white (hydrogen). The dotted lines indicate possible intermolecular hydrogen bonding interactions.

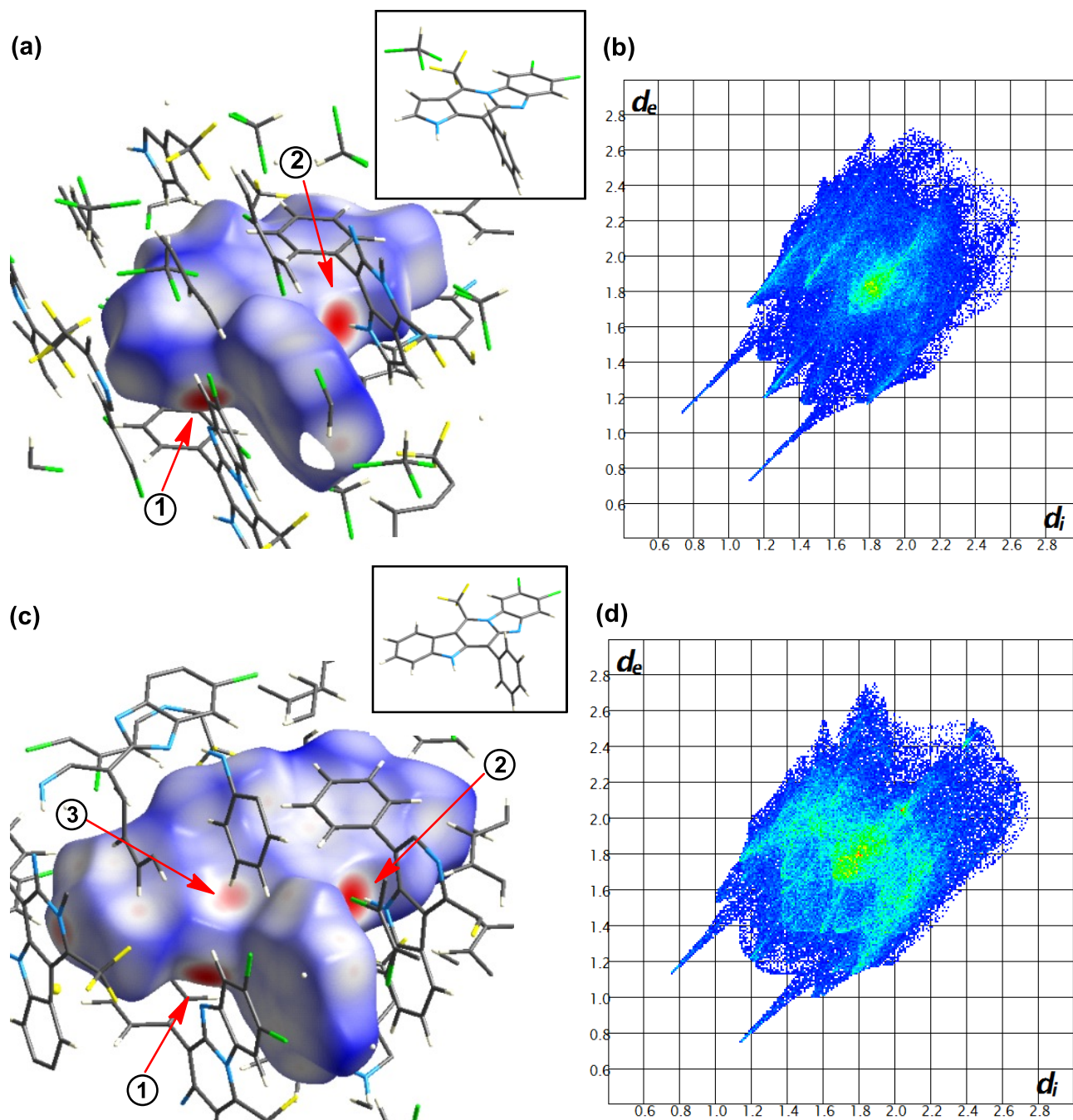
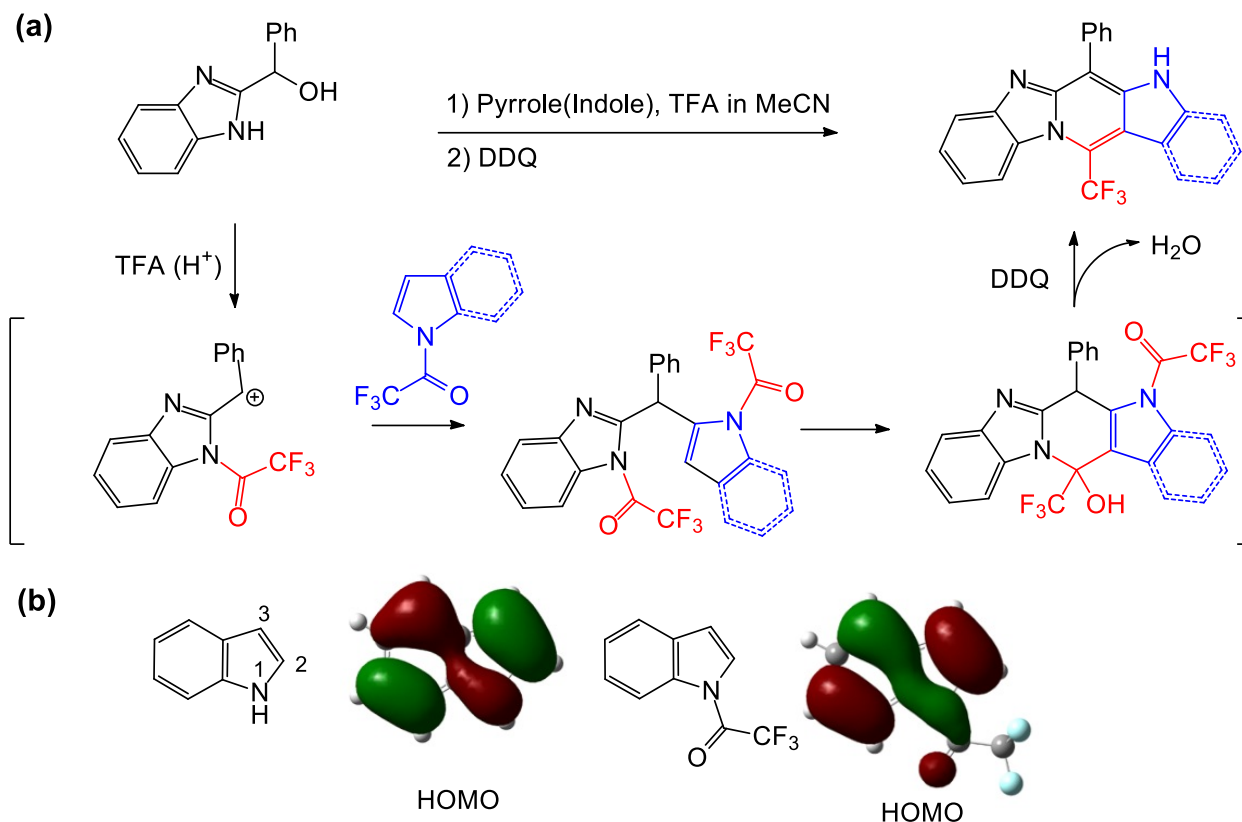


Figure S4. Crystal packing for (a) **1**•CHCl₃ and (c) **2**, showing the Hirshfeld surfaces of the central molecules mapped with d_{norm} . The inset shows the underlying structure of the central molecules. The most significant intermolecular interactions are: (1) N-H•••N(imidazole) hydrogen bond; (2) N(amide)-H•••N(imidazole) hydrogen bond; (3) C(arene)-H•••C (arene) π -interaction. The fingerprint plots for **1** and **2** are shown in (b) and (d), respectively.



Scheme S1. (a) Possible mechanism accounting for the formation of **1** via a cascade-type reaction sequence involving an acid-catalyzed condensation, formation of an amide-linkage, and oxidative dehydrogenation followed by hydrolysis of the amide linkage. (b) HOMOs of indole (left) and *N*-trifluoroacetoxyindole (right) obtained from B3LYP/6-31G(d,p) calculations, which serve to confirm the relatively large electron densities present at the C-2 positions.

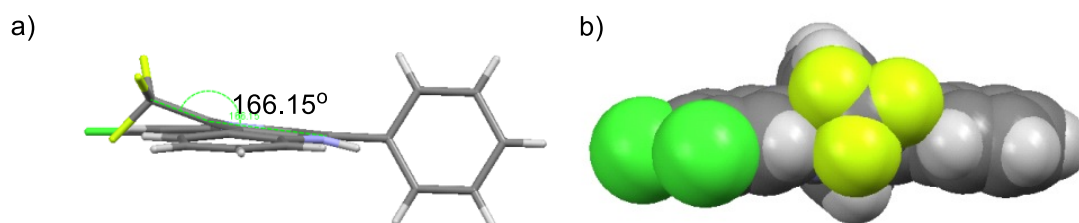


Figure S5. Out of core plane orientation of the trifluoromethyl group present in **2**; a) schematic side view (the indicated value is the bite angle between the central pyridine ring and the axis of the trifluoromethyl group), and (b) the side view given in a space filling representation.

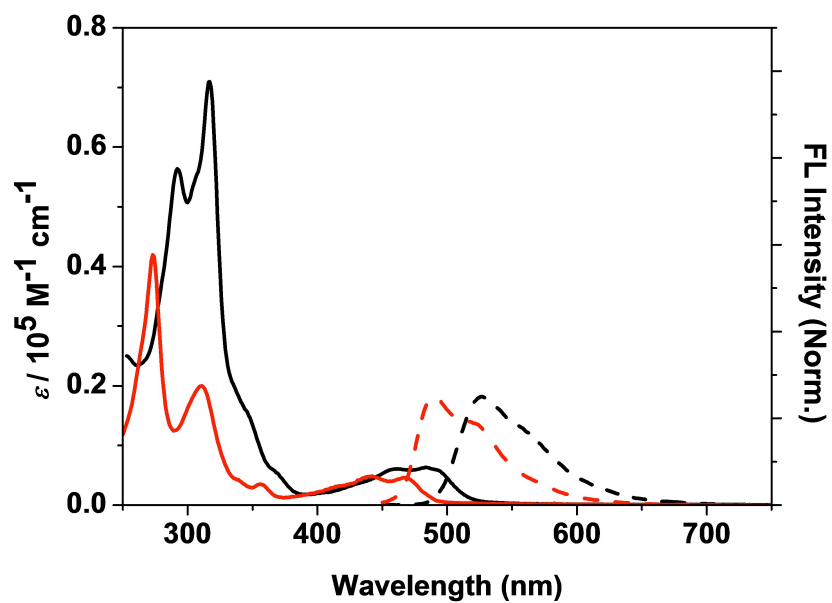


Figure S6. Steady state absorption (solid line) and fluorescence (broken line) spectra of **1** (red) and **2** (black) recorded in CH_2Cl_2 . Excitation wavelengths are 310 and 320 nm for **1** and **2**, respectively.

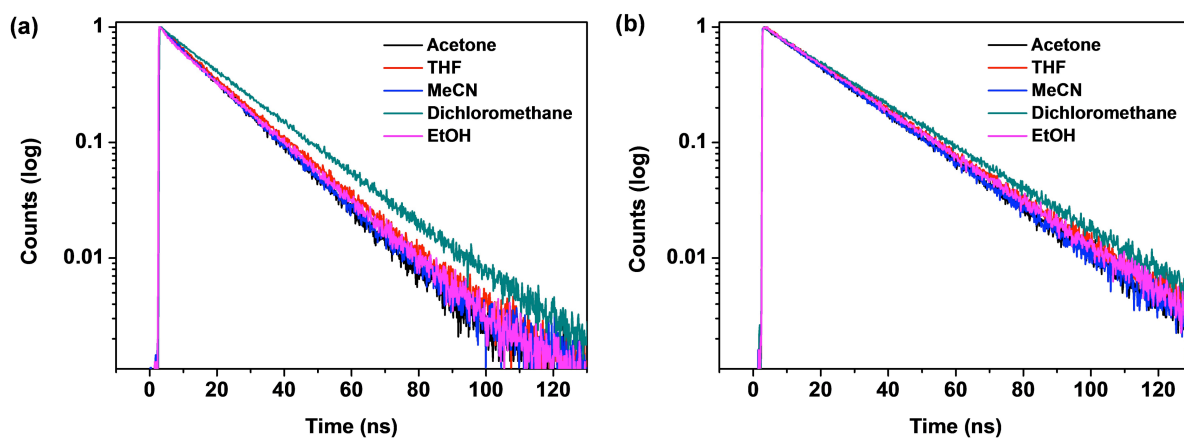


Figure S7. Fluorescence lifetime decay profiles of (a) **1** and (b) **2** recorded in acetone (black), THF (red), MeCN (blue), CH₂Cl₂ (green) and EtOH (purple) using the TCSPC method with an excitation wavelength of 370 nm. All fluorescence decay profiles were recorded at their respective fluorescence maxima.

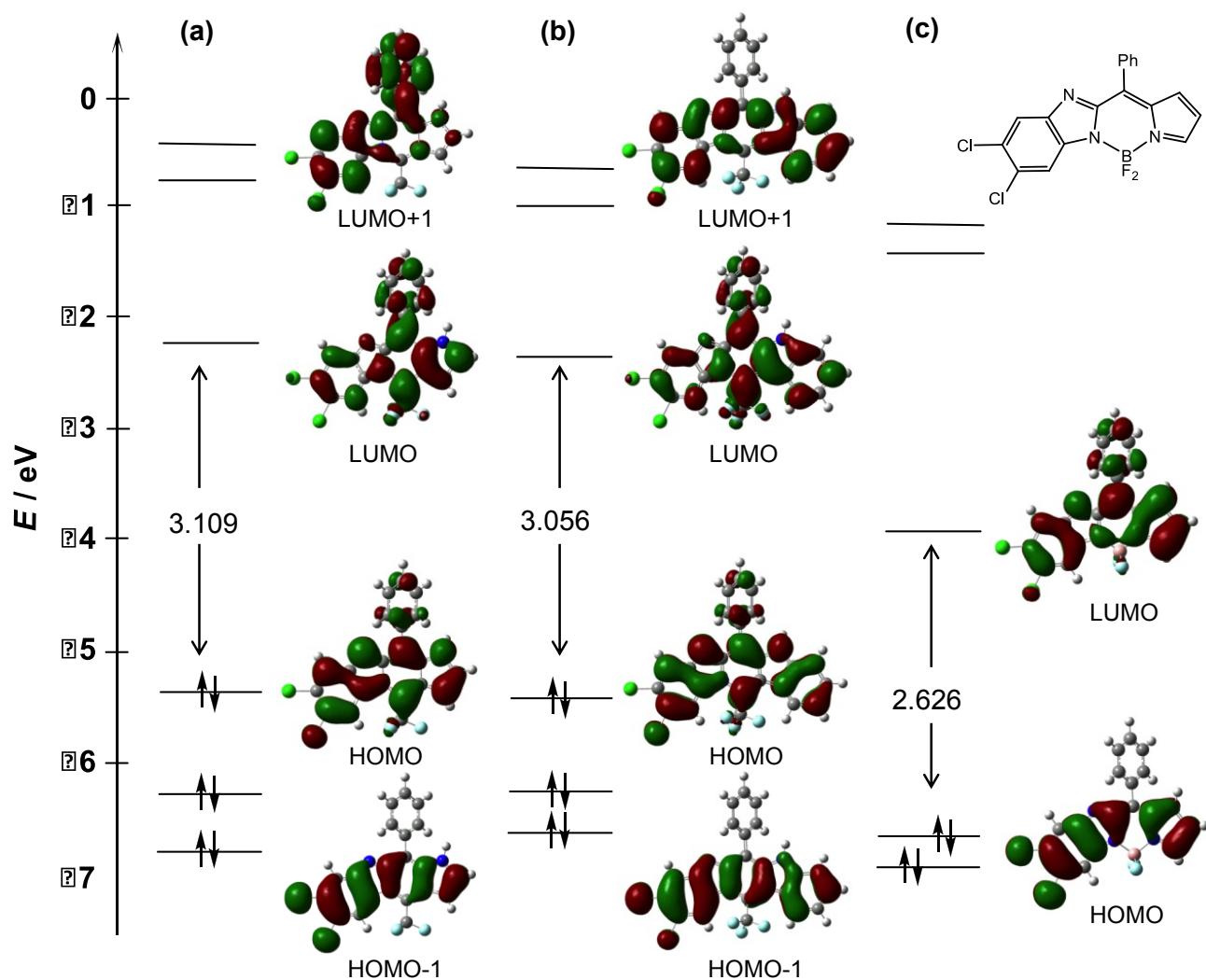


Figure S8. MO energy diagrams of (a) **1**, (b) **2** and (c) an analogous boron difluoride (BODIPY) complex calculated at the B3LYP/6-31G(d,p) levels. Note: The chemical structure of the latter species is shown at the top of the figure.

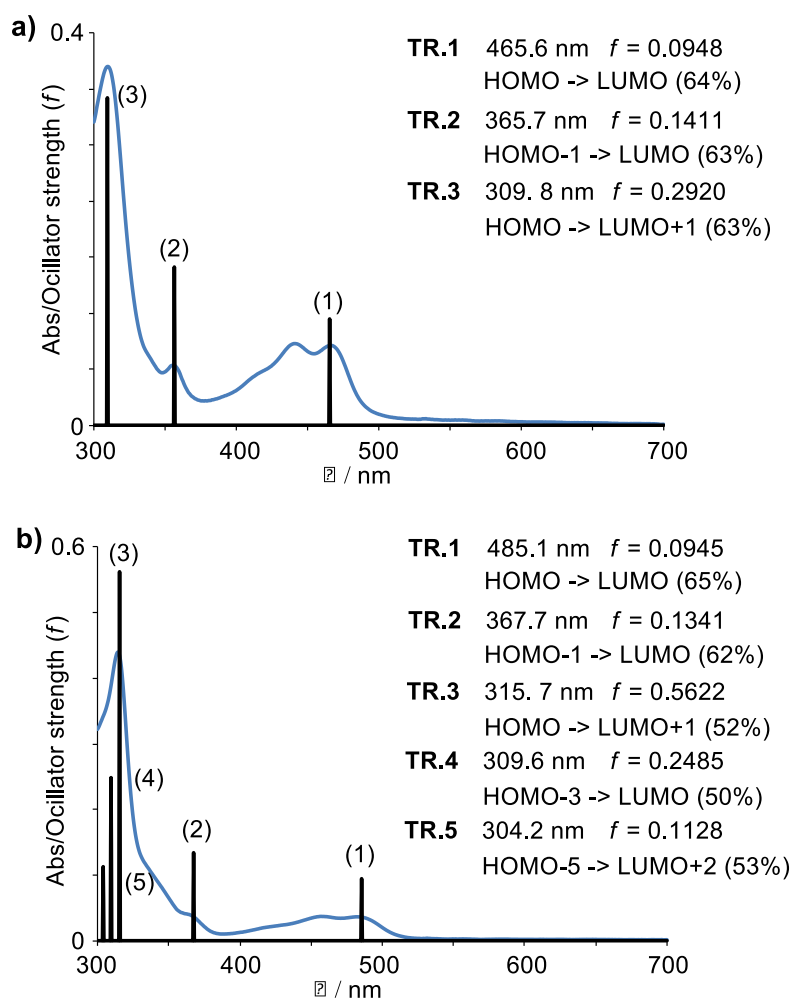


Figure S9. TDDFT stick spectra of (a) **1** and (b) **2** calculated at the B3LPY/6-31+G(d,p) level. Also shown are the UV-visible absorption spectra of **1** and **2** recorded in CH₂Cl₂. The insets list the major transition energies, oscillator strengths (f) and contributions.

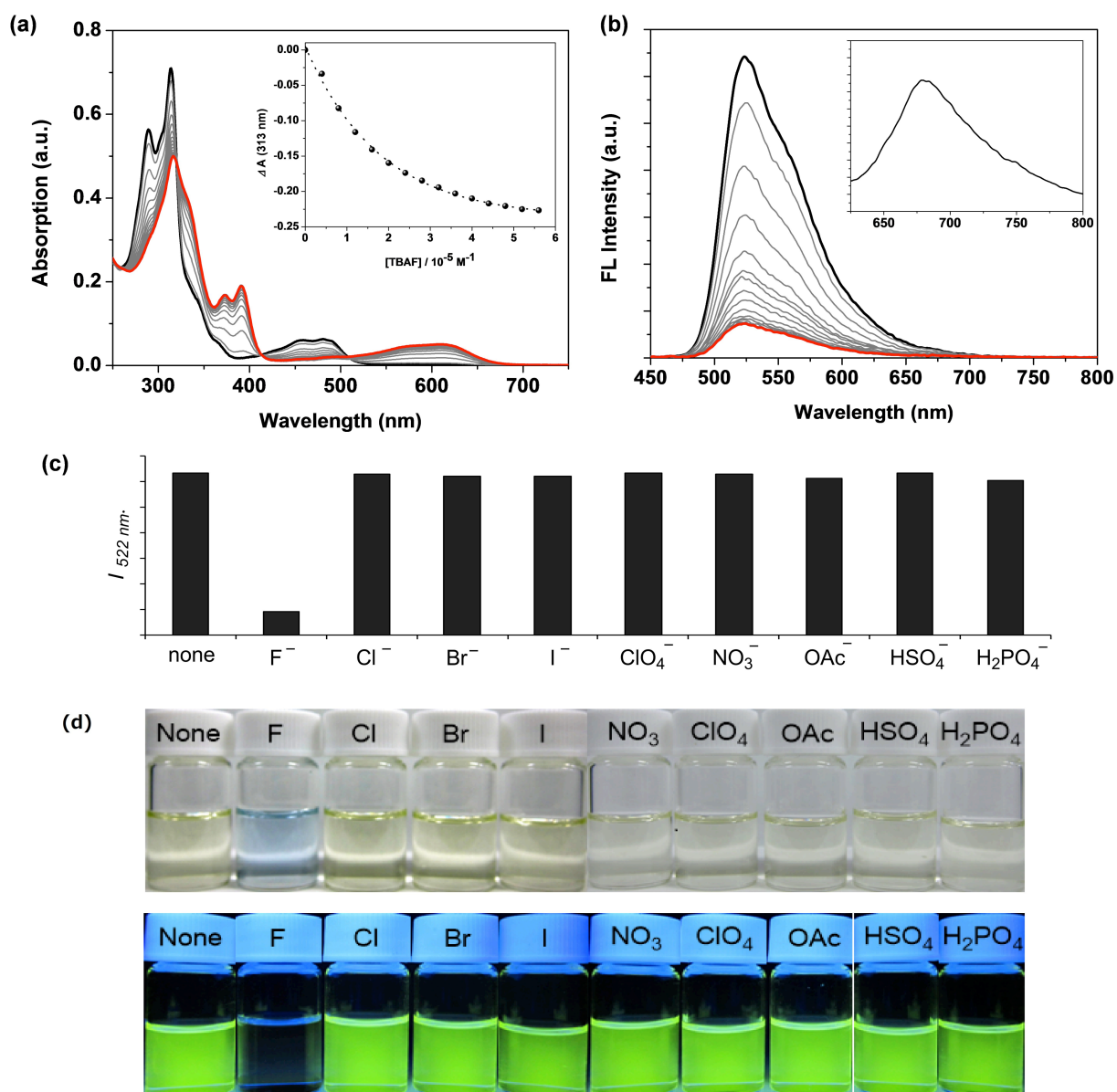


Figure S10. (a) UV-vis absorption and (b) fluorescent spectral changes of **2** (1.0×10^{-5} M) in MeCN seen upon the addition of TBAF (red: final spectrum). $\lambda_{ex} = 410$ nm. The inset to panel (a) shows the plot of the absorbance at 313 nm versus the concentration of TBAF, while the inset to panel (b) shows fluorescence spectrum observed upon excitation at 620 nm. (c) Fluorescence response ($\lambda_{em} = 552$ nm) of **2** to various TBA salts seen in MeCN (from left to right: **2** only; **2** + F^- ; **2** + Cl^- ; **2** + Br^- ; **2** + I^- ; **2** + NO_3^- ; **2** + ClO_4^- ; **2** + OAc^- ; **2** + HSO_4^- ; **2** + $H_2PO_4^-$). (d) Photos of MeCN solutions of **2** recorded after the addition of 30 equiv of the various tetrabutylammonium salts; top, under ambient light and bottom, under UV-lamp; 365 nm excitation.

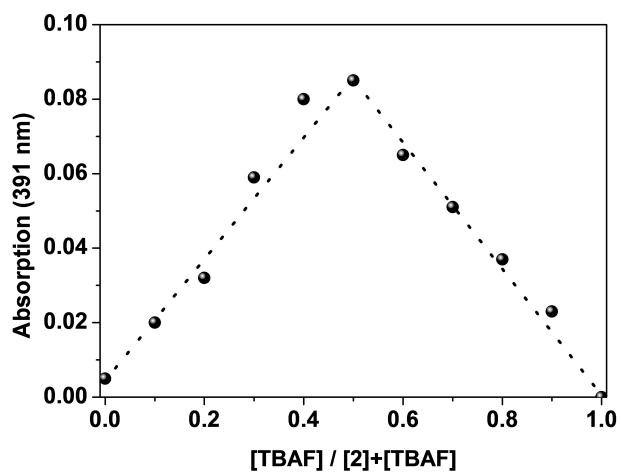
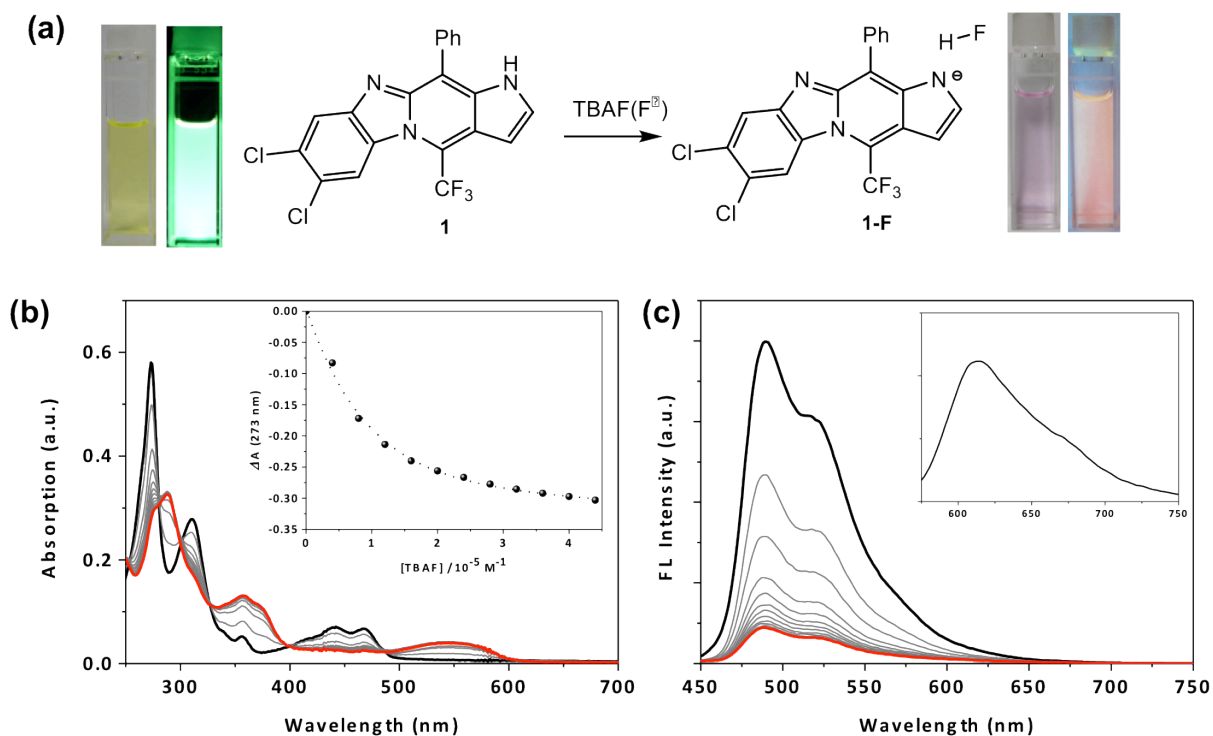


Figure S11. Job plot of the deprotonated complex, designated, **2-F**, formed by the addition of TBAF to a MeCN solution of **2**.



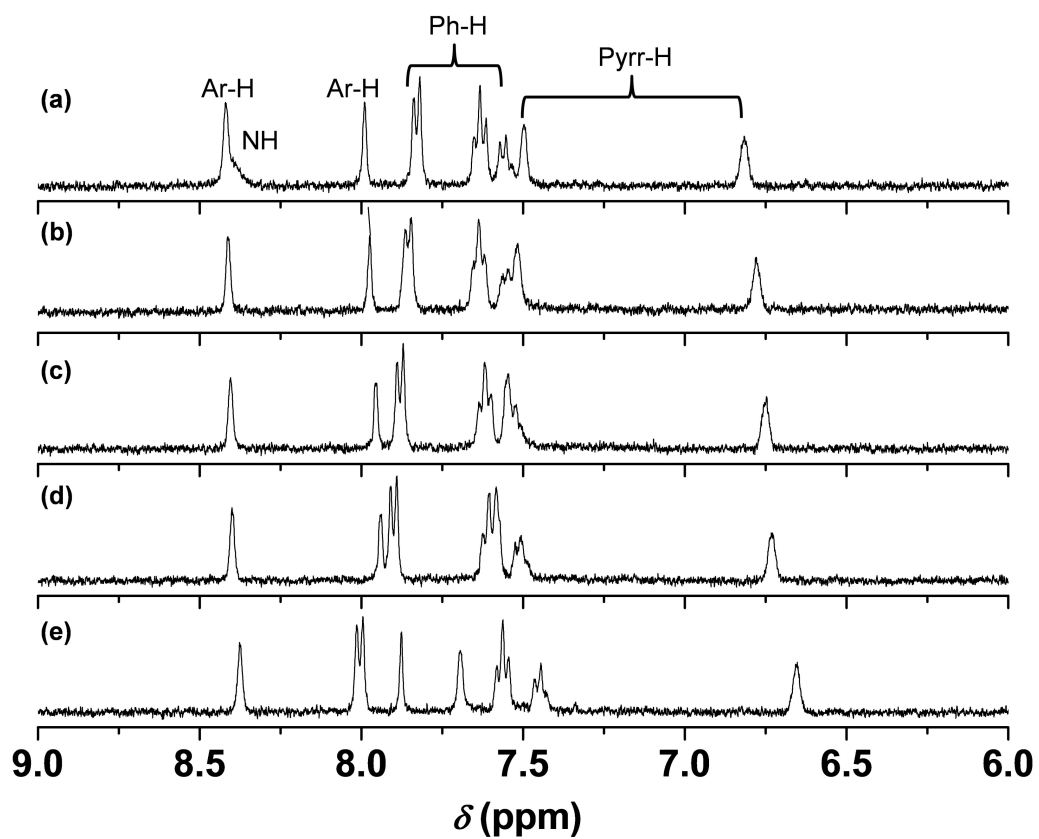


Figure S13. Partial $^1\text{H-NMR}$ spectra of **1** in CD_2Cl_2 in the various equivalent of TBAF (a) 0 equiv. (b) 1.0 equiv, (c) 2.0 equiv, (d) 3.0 equiv and (e) 5.0 equiv.

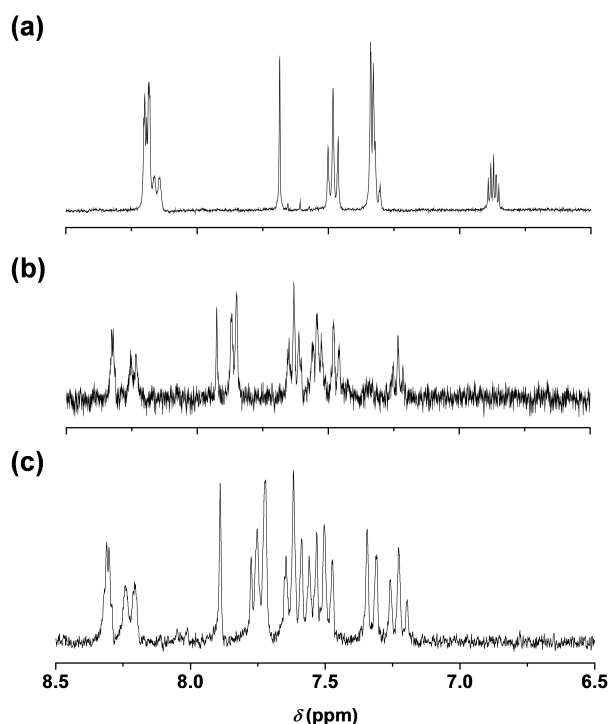


Figure S14. Partial $^1\text{H-NMR}$ spectra of (a) **2-F** in CD_3CN prepared by adding 5 equiv of TBAF to a solution of **2** in CD_3CN , and (b) the same solution after bubbling with CO_2 gas. (c) The $^1\text{H-NMR}$ spectrum of **2** recorded in CD_2Cl_2 is shown for comparison.

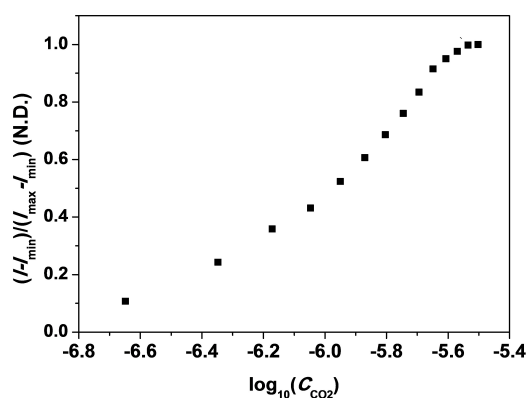


Figure S15. Fluorescence intensity change of **2** ($10.0 \mu\text{M}$) observed upon first adding 4 equiv of TBAF and then bubbling with various quantities of CO_2 ; I_{min} represent the fluorescence intensity (at 522 nm) of **2-F**; I_{max} represent the fluorescence intensity of **2-F** after bubbling with 1.3 mL of CO_2 .

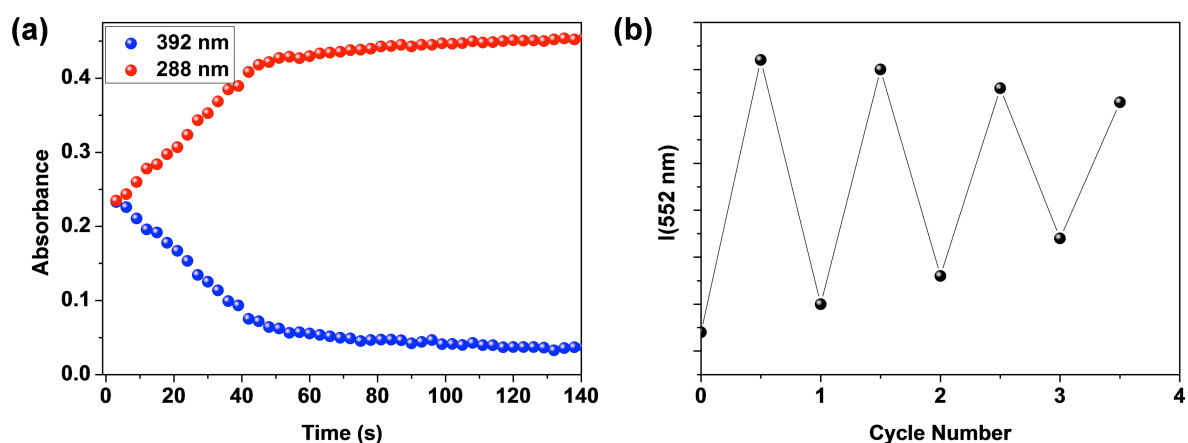


Figure S16. (a) Time course for the absorption changes of **2-F** monitored at 392 nm (blue) and 288 nm (red) upon providing a sealed cuvette with a head gas consisting of 1 atm CO_2 but not subjecting it to bubbling or deliberate mixing. (b) The change in fluorescence intensity at 552 nm associated with the deprotonation/recovery cycles of **2** that correspond to repeated treatment with TBAF followed by CO_2 bubbling.

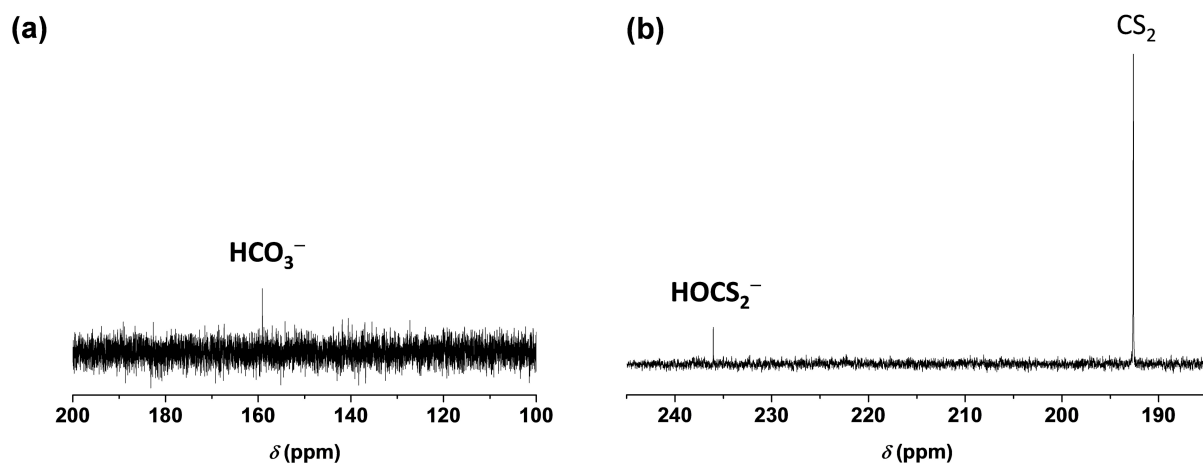


Figure S17. Partial ^{13}C -NMR spectra of (a) a solution of **2-F** in $\text{DMSO-}d_6$ after bubbling with CO_2 gas recorded in and (b) of **2-F** in $\text{DMSO-}d_6$ after reaction with CS_2 (excess).

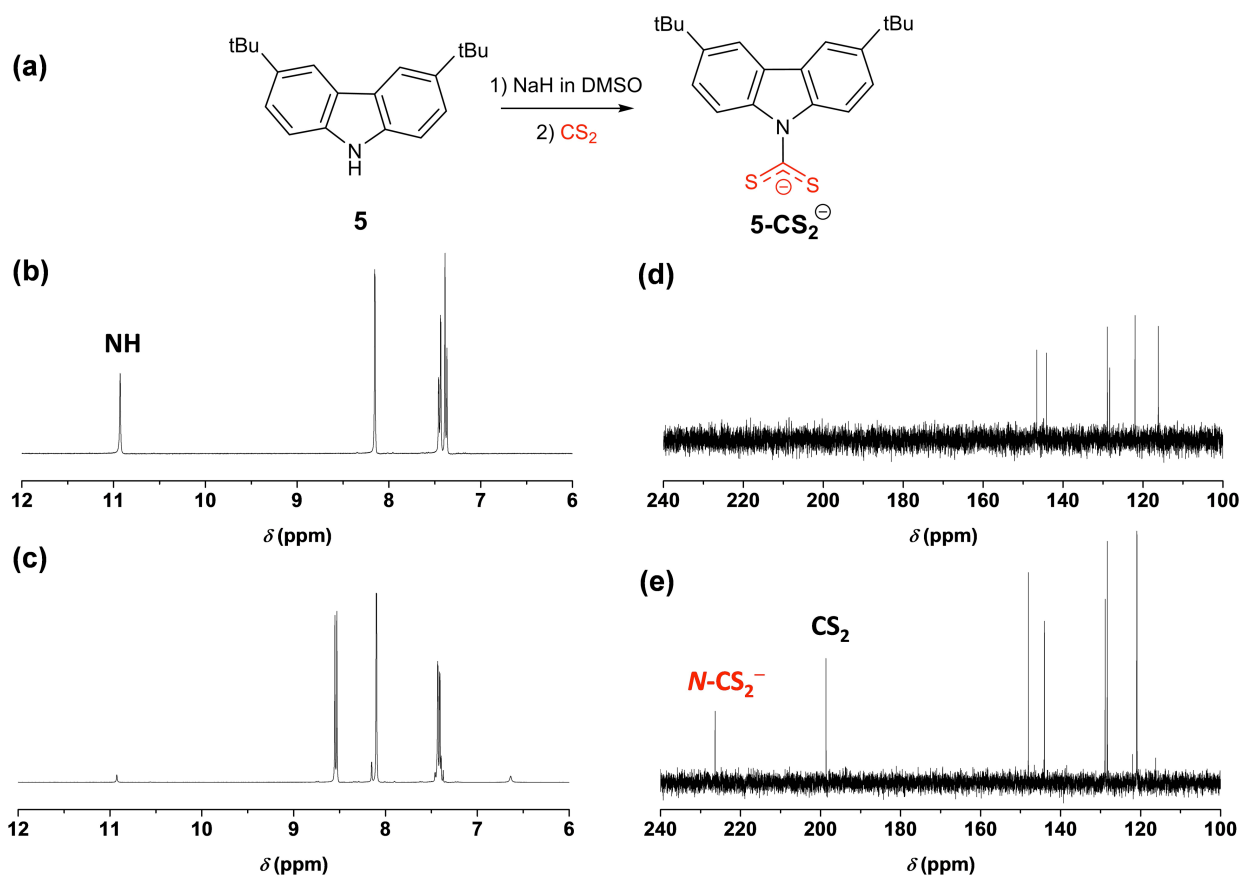


Figure S18. (a) Scheme showing the proposed formation of the CS_2 adduct of di-*tert*-Bu-carbazole^{S8} (5-CS_2). Partial $^1\text{H-NMR}$ spectra of (b) neutral 5 and (c) 5-CS_2 ; $^{13}\text{C-NMR}$ spectra of (d) 5 and (e) 5-CS_2 recorded in $\text{DMSO-}d_6$ at 298K.

References

1. M. Gökçe, S. Utku, S. Gür, A. Özkul, F. Gümüş, *Eur. J. Med. Chem.* **2005**, *40*, 135.
2. CrystalStructure 4.0: Crystal Structure Analysis Package, Rigaku and Rigaku/MSC, The Woodlands, USA Rigaku, Japan.
3. M.A. Spackman, D. Jayatilaka, *CrystEngComm*, **2009**, *11*, 19.
4. M.A. Spackman, J.J. McKinnon, *CrystEngComm*, **2002**, *4*, 378.
5. M. J. Frisch, G. W. Trucks, H. B. Schlegel, G. E. Scuseria, M. A. Robb, J. R. Cheeseman, J. A. Montgomery, Jr., T. Vreven, K. N. Kudin, J. C. Burant, J. M. Millam, S. S. Iyengar, J. Tomasi, V. Barone, B. Mennucci, M. Cossi, G. Scalmani, N. Rega, G. A. Peterson, H. Nakatsuji, M. Hada, M. Ehara, K. Toyota, R. Fukuda, J. Hasegawa, M. Ishida, T. Nakajima, Y. Honda, O. Kitao, H. Nakai, M. Klene, X. Li, J. E. Knox, H. P. Hratchian, J. B. Cross, C. Adamo, J. Jaramillo, R. Gomperts, R. E. Stratmann, O. Yazyev, A. J. Austin, R. Cammi, C. Pomelli, J. W. Ochterski, P. Y. Ayala, K. Morokuma, G. A. Voth, P. Salvador, J. J. Dannenberg, V. G. Zakrzewski, S. Dapprich, A. D. Daniels, M. C. Strain, O. Farkas, D. K. Malick, A. D. Rabuch, K. Raghavachari, J. B. Foresman, J. V. Ortiz, Q. Cui, A.G. Baboul, S. Clifford, J. Cioslowski, B. B. Stefanov, G. Liu, A. Liashenko, P. Piskorz, I. Komaromi, R. L. Martin, D. L. Fox, T. Keith, M. A. Al-Laham, C. Y. Peng, A. Nanayakkara, M. Challacombe, P. M. W. Gill, B. Johnson, W. Chen, M. W. Wong, C. Gonzalez, J. A. Pople, Gaussian 03, Revision B.05, Gaussian, Inc., Pittsburgh, PA (USA), **2003**.
6. a) A. D. Becke, *Phys. Rev. A* **1988**, *38*, 3098; b) C. Lee, W. Yang, R. G. Parr, *Phys. Rev. B* **1988**, *37*, 785; c) A.D. Becke, *J. Chem. Phys.* **1993**, *98*, 5648.
7. R. F. Kubin and A. N. Fletcher, *J. Lumin.*, **1982**, *27*, 455.
8. Z. Merican, T. L. Schiller, C. J. Hawker, P. M. Fredericks, I. Blakey, *Langmuir*, **2007**, *23*, 10539.